JOURNAL OF VIROLOGY, Oct. 2011, p. 10222–10229 Vol. 85, No. 19
0022-538X/11/$12.00 doi:10.1128/JVI.00691-11

Functional Interactions between Polydnavirus and Host Cellular Innexins[▽]

N. K. Marziano,[1]†‡ D. K. Hasegawa,[2]† P. Phelan,[1]* and M. W. Turnbull[2,3]*

School of Biosciences, University of Kent, Canterbury, Kent, United Kingdom[1]; Department of Biological Sciences, Clemson University, Clemson, South Carolina[2]; and School of Agricultural, Forest, and Environmental Sciences, Clemson University, Clemson, South Carolina[3]

Received 5 April 2011/Accepted 21 July 2011

Polydnaviruses are double-stranded DNA viruses associated with some subfamilies of ichneumonoid parasitoid wasps. Polydnavirus virions are delivered during wasp parasitization of a host, and virus gene expression in the host induces alterations of host physiology. Infection of susceptible host caterpillars by the polydnavirus *Campoletis sonorensis* ichnovirus (CsIV) leads to expression of virus genes, resulting in immune and developmental disruptions. CsIV carries four homologues of insect gap junction genes (innexins) termed vinnexins, which are expressed in multiple tissues of infected caterpillars. Previously, we demonstrated that two of these, VinnexinD and VinnexinG, form functional gap junctions in paired *Xenopus* oocytes. Here we show that VinnexinQ1 and VinnexinQ2, likewise, form junctions in this heterologous system. Moreover, we demonstrate that the vinnexins interact differentially with the Innexin2 orthologue of an ichnovirus host, *Spodoptera frugiperda*. Cell pairs coexpressing a vinnexin and Innexin2 or pairs in which one cell expresses a vinnexin and the neighboring cell Innexin2 assemble functional junctions with properties that differ from those of junctions composed of Innexin2 alone. These data suggest that altered gap junctional intercellular communication may underlie certain cellular pathologies associated with ichnovirus infection of caterpillar hosts.

Polydnaviruses (PDVs) are double-stranded DNA viruses obligatorily associated with certain parasitoid wasps. The viruses exist in proviral state in the germ line nuclear genome of braconid and ichneumonid wasps and are recognized according to wasp associate as bracoviruses (BVs) and ichnoviruses (IVs), respectively. Although the two lineages are unrelated evolutionarily (6, 58), they grossly share similar life cycles and symptoms of infection. PDV virions are produced in the ovaries of pupal and adult female wasps and are delivered into the host, typically an immature lepidopteran (caterpillar), during parasitization (21, 55). Expression of virus genes results in numerous physiological alterations in the host, including disruption of host humoral and cellular immune responses. Notably, encapsulation, a multicellular immune response and the primary antiparasitoid defense, is typically disrupted (5, 25, 38, 47).

PDV genomes comprise large gene numbers, typically occurring in multiple-member gene families (16, 33, 53, 60). The genome of *Campoletis sonorensis* ichnovirus (CsIV) contains five gene families, cysteine motif, vankyrin, repeat element, N family, and vinnexin, and a putative sixth family, encoding polar-residue-rich proteins (53, 60). While the cysteine motif (12, 36) and vankyrin (31, 32) proteins have been linked to disruption of host immunity, the roles of the other gene families have not been reported. The vinnexins (Vnx) are homologous to the innexins (54, 55), one of two gene families which encode the structural units of gap junctions.

Innexins (Inx; also known as pannexins) compose gap junctions in insects and other prechordates; they persist in small numbers in higher organisms, where the bulk of gap junctions are formed from members of the unrelated connexin family (7, 24, 40, 42, 64, 66). Gap junctions consist of paired hemichannels which interact to bridge the intercellular gap between appositional membranes of two cells. Hemichannels, in turn, can comprise either a single or multiple innexin (or connexin) proteins; the former is referred to as a homomeric, and the latter a heteromeric, channel. Additionally, apposing hemichannels may be homotypic (hemichannels of identical composition) or heterotypic (composition of the hemichannels differs). Studies of both innexin (7, 22, 41, 49, 50) and connexin (1, 28, 63, 67) channels in *in vitro* expression systems have demonstrated that the specific subunit composition influences the conductance of the channel and its sensitivity to regulatory factors, such as voltage (11, 40). *In vivo* studies have found no evidence for extensive functional redundancy in either family of gap junction proteins; in many cases, innexins and connexins are unable to complement loss-of-function mutations in paralogues (13, 23, 35, 62, 65, 68). Thus, the precise molecular makeup of gap junction channels is an important determinant of their functional properties.

Four vinnexins, VnxD, VnxG, VnxQ1, and VnxQ2, are encoded by the CsIV genome (60). All are transcribed in multiple tissues of infected caterpillars, and VnxQ2 forms junctional plaques at appositional membranes of infected cells (54). Innexin2 (Inx2), one of the most highly conserved members of the insect innexin gene family, is expressed throughout lepi-

* Corresponding author. Mailing address for P. Phelan: School of Biosciences, University of Kent, Canterbury, Kent, United Kingdom CT2 7NJ. Phone: 44 1227 823002. Fax: 44 1227 763912. E-mail: P.Phelan@kent.ac.uk. Mailing address for M. W. Turnbull: 113 Long Hall Box 340315, School of Agricultural, Forest, and Environmental Sciences, Clemson University, Clemson, SC 29634-0315. Phone: (864) 656-5038. Fax: (864) 656-0274. E-mail: turnbul@clemson.edu.

‡ Present address: School of Life Sciences, University of Sussex, United Kingdom.

† Contributed equally to the work.

▽ Published ahead of print on 3 August 2011.

dopteran larval stages in similar tissues (29, 44). Therefore, there is scope for vinnexins to form *de novo* gap junctions and/or to interact with cellular innexins in infected host tissues. Consequent alterations in intercellular communication could contribute to the physiological changes in the host that are necessary for survival of the parasite.

Previously, we demonstrated that CsIV VnxD (CsIV-VnxD) and CsIV-VnxG form functional gap junctions when expressed in paired *Xenopus* oocytes (54). Here we have used the same system, first, to assess the channel-forming ability of CsIV-VnxQ1 and CsIV-VnxQ2. Second, we have tested the ability of Inx2 from a lepidopteran host of ichnoviruses, *Spodoptera frugiperda*, to form gap junctions. Finally, we have coexpressed the vinnexins and *S. frugiperda* Inx2 (*Sf*-Inx2) in heteromeric and heterotypic configurations to determine whether virus and host proteins are capable of interacting and how such interactions influence the properties of gap junctions. We establish that all four Vnxs are functional gap junction proteins. The Vnxs differentially interact with Inx2 to give rise to channels with novel properties.

MATERIALS AND METHODS

Synthesis of constructs for *in vitro* expression. *CsIV-vnxD* and *CsIV-vnxG* were subcloned into the pSPJC2L expression vector for expression in *Xenopus* oocytes, as previously described (54). Similar methods were used to generate *CsIV-vnxQ1*-pSPJC2L, *CsIV-vnxQ2*-pSPJC2L, and *Sf-Inx2*-pSPJC2L. *CsIV-vnxQ1* was PCR amplified from CsIV genomic DNA (courtesy of Bruce Webb, University of Kentucky) using the primers 5′-CCCATATGAACGCACCATGCTCAAGA and 5′-GCCATATGATTAGACACAGTTACAAT; *CsIV-vnxQ2* was amplified using the primers 5′-CTAGATCTCTTCATACTGTTCACGATG and 5′-CATCATATGGTAAATCATGTCAAACG. *Sf-inx2* was amplified from Sf9 cDNA, synthesized from DNase I-treated total RNA isolated from Sf9 cells, using the primers 5′-ATAAGCTTGCCATGTTTGACGTATTC and 5′-GAATTCGACTACACACTGTCCTTCC. Amplimers were cloned into pGEM-T Easy (Promega), sequenced, and subcloned into pSPJC2L using the underlined restriction site. 5′-capped, poly(A) RNA was synthesized as previously described (54) and verified by spectrophotometry, gel electrophoresis, and *in vitro* translation by rabbit reticulocyte assay (Ambion).

Expression of innexin and vinnexin RNAs in paired *Xenopus* oocytes. The isolation, microinjection, and pairing of oocytes were performed essentially as described previously (41, 42, 52). In brief, *Xenopus laevis* oocytes were incubated in Ca^{2+}-free Barth's medium (10) containing 1 mg/ml each of collagenase (Roche Diagnostics) and hyaluronidase (Sigma-Aldrich) for 30 to 60 min. Following exposure to protease inhibitors, stage V to VI oocytes were defolliculated using a pair of fine forceps. Isolated cells were firstly preinjected (Nanoject injector; Drummond) with 20 ng *Xenopus* connexin 38 DNA antisense oligonucleotide (42) to prevent any endogenous coupling. After an approximately 18-h incubation period, oocytes were microinjected with 2 to 10 ng *Sf-inx2* or *vinnexin* mRNA, alone or in combination, in 20 nl RNase-free H_2O. Alternatively, cells were injected with H_2O alone as a control. Oocytes were then exposed to a hypertonic medium to aid the removal of the vitelline envelope, paired, and incubated in Barth's medium at 20°C for 24 to 48 h. Potential coupling between paired oocytes was recorded using the dual voltage clamp technique (48) with borosilicate glass electrodes filled with recording solution (42). Data acquisition and analysis were carried out using pClamp 9.0 software (Axon Instruments). Junctional conductance (Gj) and its relationship to transjunctional voltage (Vj) were determined using previously described protocols (56). Plots of Gj versus Vj were made in Origin 7 (OriginLab). Where possible, data were fitted to a Boltzmann equation, $y = A2 + A1 - A2/\{1 + \exp[(x - x0)/dx]\}$, where $A1$ and $A2$ are maximum (Gj_{max}) and minimum (Gj_{min}) conductances, respectively, $x0$ is the voltage at which conductance is halfway between its maximum and minimum values (V0), and dx represents the change in conductance over the voltage range, a measure of voltage sensitivity.

Xenopus laevis was maintained according to approved Clemson University Institutional Animal Care and Use Committee protocols.

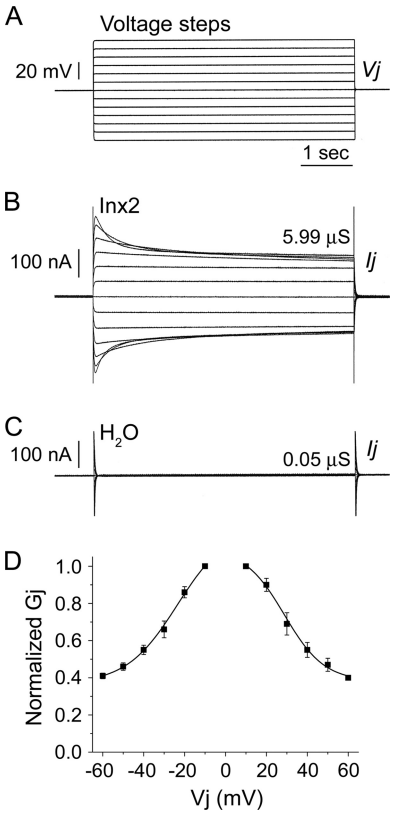

FIG. 1. *Spodoptera frugiperda* Inx2 forms functional, voltage-dependent gap junction channels *in vitro*. *Xenopus laevis* oocytes were microinjected with 2 to 5 ng *Sf-inx2* mRNA or water as a negative control. Following removal of the vitelline membranes, cells were paired and potential coupling was assessed 24 to 48 h later using the dual voltage clamp technique. Each cell of the pair was initially clamped to a holding potential (Vh) of −80 mV. Sequential depolarizing and hyperpolarizing voltage steps (A) were then applied to one cell of the pair (V1) while the second cell was maintained at Vh, generating a transjunctional potential difference, Vj (V1 − Vh, mV). The current Ij GAY required to maintain cell 2 at Vh was recorded and the transjunctional conductance, Gj (μS), calculated as Ij/Vj. (B) Representative trace for a cell pair expressing *Sf-inx2* mRNA. The channels display sensitivity to transjunctional voltage, observed by the decrease in the currents with increasing depolarization and hyperpolarization. (C) No currents were recorded from water-injected controls, indicating that these cell pairs are not electrically coupled. (D) Gj/Vj plot showing the steady-state Gjs recorded in response to Vj steps applied to Inx2-expressing cell pairs. Gjs are normalized to their values at ±10 mV and are shown as mean ± SEM ($n = 4$ pairs). Data are fitted to a Boltzmann equation (parameters in text).

RESULTS

***Spodoptera frugiperda* Inx2 forms homotypic gap junction channels in paired *Xenopus* oocytes.** The ability of Inx2 from *Spodoptera frugiperda*, a lepidopteran host of the ichnoviruses, to form functional homotypic gap junction channels was assessed following expression of this protein in *Xenopus laevis* oocytes. Oocytes were microinjected with 2 to 5 ng *Sf-inx2* mRNA, and electrical coupling between paired cells was measured 24 to 48 h later. High levels of electrical coupling were observed between virtually all cell pairs recorded (97% of pairs coupled) (Fig. 1A and B). The average junctional conductance for these homotypic channels was found to be 18.99 ± 1.92 μS

TABLE 1. Expression of *Sf*-Inx2 and CsIV vinnexin proteins in homomeric, heteromeric, and heterotypic configuration in paired *Xenopus* oocytes[a]

Cell 1/cell 2	Pairs coupled/total (%)	Mean Gj (μS) ± SEM	*n*
Inx2/Inx2	36/37 (97)	18.99 ± 1.92	36
VnxD/VnxD	12/22 (55)	1.36 ± 0.30	12
VnxG/VnxG	11/11 (100)	8.02 ± 2.50	11
VnxQ1/VnxQ1	4/16 (25)	1.37 ± 0.43	4
VnxQ2/VnxQ2	28/38 (74)	2.52 ± 0.30	28
Inx2+VnxD/Inx2+VnxD	25/28 (89)	4.93 ± 1.20	25
Inx2+VnxG/Inx2+VnxG	18/18 (100)	19.62 ± 2.56	18
Inx2+VnxQ1/Inx2+VnxQ1	18/20 (90)	8.60 ± 2.02	18
Inx2+VnxQ2/Inx2+VnxQ2	31/35 (89)	16.49 ± 2.28	31
Inx2/VnxD	5/20 (25)	0.94 ± 0.24	5
Inx2/VnxG	12/13 (92)	12.48 ± 3.68	12
Inx2/VnxQ1	1/8 (13)	1.23	1
Inx2/VnxQ2	5/12 (42)	0.82 ± 0.37	5
H_2O/H_2O	0/91 (0)	0.20 ± 0.02	91

[a] Cell pairs were recorded using a dual voltage clamp technique as described in the legend for Fig. 1. Junctional conductances (Gj) were calculated at a Vj of ±10 mV and are shown as mean ± SEM for coupled pairs (*n*). The percentage of coupled pairs, from the total recorded, is shown in parentheses.

(mean ± standard error of the mean [SEM], $n = 36$) (Table 1). No electrical coupling was observed between paired cells microinjected with water alone (Fig. 1A and C).

Inx2 channels were found to be voltage sensitive, shown by the steady decrease in the currents with increasing depolarizing or hyperpolarizing voltage steps (Fig. 1B). This indicates a reduction in the opening probability of the channels with increasing transjunctional potential difference (Vj). To examine further this voltage response, the normalized steady-state junctional conductance (Gj) at each voltage step was calculated and plotted against Vj. The data fitted well to a single Boltzmann equation (Fig. 1D). From the Gj/Vj plot and calculated Boltzmann parameters, it can be seen that the channels display a symmetrical response to applied voltage. For hyperpolarizing Vjs, Gj_{max} is 1.22 ± 0.24, Gj_{min} is 0.37 ± 0.05, and V0 is −23.55 ± 7.18; the corresponding values for depolarizing Vjs are Gj_{max} of 1.1 ± 0.13, Gj_{min} of 0.38 ± 0.06, and V0 of 28.8 ± 4.19.

***Campoletis sonorensis* ichnovirus vinnexin proteins VnxQ1 and VnxQ2 form homotypic gap junction channels in paired *Xenopus* oocytes.** Two CsIV vinnexin proteins, VnxD and VnxG, have previously been shown to form functional homotypic gap junction channels in paired *Xenopus* oocytes (54). These findings were confirmed in the present study. Fifty-five percent of the VnxD-expressing cell pairs were found to be electrically coupled, with an average Gj value of 1.36 ± 0.3 μS (mean ± SEM, $n = 12$) (Table 1), a value similar to that previously reported (54). All cell pairs injected with *vnxG* were found to be coupled, with an average Gj value of 8.02 ± 2.5 μS (mean ± SEM, $n = 11$) (Table 1), a conductance slightly higher than the previously reported value (54). As previously observed (54), VnxD and VnxG homotypic channels were voltage insensitive (data not shown).

The channel-forming capabilities of the remaining two CsIV vinnexins, VnxQ1 and VnxQ2, were similarly assessed in paired *Xenopus* oocytes following the microinjection of 5 to 10 ng *vnx* mRNA. Electrical coupling was observed in 25% of cell pairs expressing VnxQ1 (Fig. 2A and B). These gap junctions displayed an average conductance of 1.37 ± 0.43 μS (mean ± SEM, $n = 4$) (Table 1). Similarly to VnxD and VnxG and unlike *Sf*-Inx2 channels, the currents recorded from VnxQ1 homotypic oocyte pairs were linear (Fig. 2B), indicating that these channels lack transjunctional voltage sensitivity.

Electrical coupling was observed between the majority of cell pairs expressing VnxQ2 (74% of pairs coupled) (Fig. 2A and C), indicating that VnxQ2 readily forms homotypic channels. The average junctional conductance of the channels was 2.52 ± 0.3 μS (mean ± SEM, $n = 28$) (Table 1). As with the other vinnexin homotypic channels, VnxQ2 channels lacked transjunctional voltage sensitivity, with linear currents recorded at all voltage steps (Fig. 2C). No coupling was observed between water-injected control cell pairs (Fig. 2D).

Effects on channel properties of *Sf*-Inx2 and CsIV vinnexin coexpression. The similarity between the endogenous insect innexins and the vinnexin proteins raises the questions of whether or not these proteins can interact and whether any such interaction results in an alteration in the properties of the insect's gap junction channels. To address these questions, a

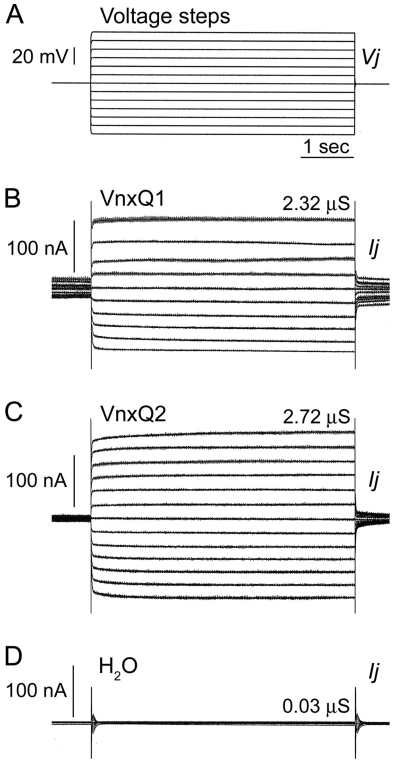

FIG. 2. *Campoletis sonorensis* ichnovirus VnxQ1 and VnxQ2 form functional gap junction channels *in vitro*. *Xenopus laevis* oocytes were microinjected with 5 to 10 ng CsIV *vnxQ1* or *vnxQ2* mRNA or water as a negative control. Cell pairs were prepared and recorded as described in the legend for Fig. 1. One cell of each pair was subjected to a series of depolarizing and hyperpolarizing voltage steps (Vj) (A), and currents (Ij) were simultaneously recorded in the other cell. (B) Representative trace for a cell pair expressing VnxQ1. Junctional conductance, Gj (Ij/Vj), is 2.32 μS. Currents are linear at all Vjs, demonstrating that VnxQ1 gap junction channels lack voltage sensitivity. (C) Representative trace for a cell pair expressing VnxQ2 mRNA. Gj is 2.72 μS. Currents are linear at all Vjs, indicating a lack of voltage sensitivity. (D) Water-injected control pairs are not coupled.

series of coexpression experiments were carried out to examine the electrical coupling between paired oocytes microinjected with both *Sf-inx2* mRNA (2 to 5 ng) and one of the four CsIV *vnx* mRNAs (2 to 5 ng). Typical current traces recorded from coinjected cell pairs and corresponding Gj/Vj plots can be seen in Fig. 3. For comparative purposes, the Gj/Vj plot for Inx2 homotypic channels is presented in each case.

Coexpression of VnxD with Inx2 (Fig. 3A to C; Table 1) resulted in a significant reduction in the junctional conductance. The average Gj value for Inx2+VnxD pairs was 4.93 ± 1.2 μS (mean ± SEM, $n = 25$), significantly lower than the average Gj of Inx2 homotypic channels ($P < 0.01$, two-sample *t* test) (Table 1). The voltage characteristics of the channels in cell pairs coinjected with Inx2 and VnxD (Fig. 3C, filled symbols) did not differ markedly from those in pairs expressing Inx2 only (Fig. 3C, open symbols); however, the heteromeric pairs showed marginally greater sensitivity to depolarizing Vjs than Inx2 homotypic pairs, resulting in slight asymmetry of the Gj-Vj response. The data, particularly for depolarizing Vjs, were not well fit by a single Boltzmann equation, possibly reflecting the presence of more than one channel type.

Coexpression of VnxG with Inx2 (Fig. 3A, D, and E) did not affect levels of conductance but did significantly alter the voltage properties of the channels. A Gj value of 19.62 ± 2.56 μS (mean ± SEM, $n = 18$) was calculated for Inx2+VnxG-expressing pairs, very similar to that of pairs expressing Inx2 alone (Table 1). However, channels in cell pairs expressing Inx2+VnxG (Fig. 3E, filled symbols) showed less sensitivity to both depolarizing and hyperpolarizing transjunctional voltages than Inx2 homotypic channels (Fig. 3E, open symbols). The Gj/Vj data fitted well to a single Boltzmann equation, indicating that the cells express a fairly homogenous population of channels. Gj_{max}, Gj_{min}, and V0, respectively, were 1.01 ± 0.02, 0.75 ± 0.12, and −42.32 ± 9.37 for hyperpolarizing potentials and 1.04 ± 0.11, 0.64 ± 0.12, and 35.55 ± 5.82 for depolarizing potentials.

Channels formed in cell pairs coexpressing VnxQ1 and Inx2 (Fig. 3A, F, and G) differed from Inx2 homotypic channels in both junctional conductance and voltage sensitivity. The average Gj value was 8.60 ± 2.02 μS (mean ± SEM, $n = 18$), significantly lower than the average Gj of Inx2 homotypic channels ($P < 0.01$, two-sample *t* test) (Table 1). The Gj/Vj plot for Inx2+VnxQ1-expressing pairs is asymmetrical (Fig. 3G, filled symbols). Channels present in these cells displayed sensitivity to hyperpolarizing Vjs similar to that for pairs expressing Inx2 only (Fig. 3G, left), and these data fitted well to a single Boltzmann equation. Sensitivity to depolarizing Vjs was greater in Inx2+VnxQ1 pairs than in Inx2 homotypic pairs (Fig. 3G, right), and the data were not well fit by a single Boltzmann equation.

In contrast to the other Vnxs, coexpression of VnxQ2 with Inx2 (Fig. 3A, H, and I) yielded channels that did not obviously differ, either in conductance or in voltage sensitivity, from Inx2 homotypic channels. The average Gj value of 16.49 ± 2.28 μS (mean ± SEM, $n = 31$) for cell pairs expressing Inx2 and VnxQ2 was similar to the mean Gj of Inx2-expressing cell pairs (Table 1). The Gj/Vj plots (Fig. 3I) indicate similar degrees of voltage sensitivity; however, unlike the Inx2 homotypic data, the data for Inx2+VnxQ2 pairs were not well fit by a single Boltzmann equation.

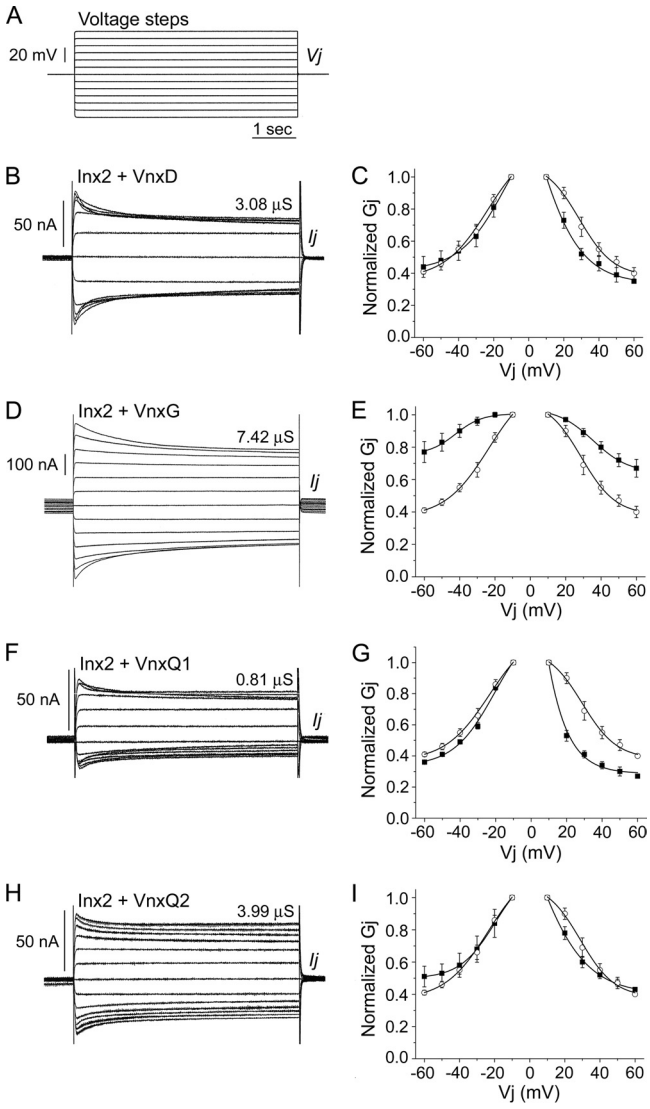

FIG. 3. Coexpression of *Sf*-Inx2 with CsIV vinnexin proteins results in gap junction channels with properties distinct from those of Inx2 or Vnx homotypic channels. *Xenopus laevis* oocytes were injected with a mix of *Sf-inx2* and one of the four CsIV *vnx* RNAs (2 to 5 ng each RNA). Cells were paired and recorded by dual voltage clamp as described in the legend for Fig. 1. A series of depolarizing and hyperpolarizing voltage steps (A) were applied to one cell of a pair and the currents induced in the neighboring cell recorded. Representative current traces (B, D, F, and H) and the corresponding Gj/Vj plots (C, E, G, and I) are shown for pairs expressing Inx2 and VnxD (B and C), Inx2 and VnxG (D and E), Inx2 and VnxQ1 (F and G), and Inx2 and VnxQ2 (H and I). In the Gj/Vj plots, Gjs are normalized to their values at ±10 mV and presented as mean ± SEM for 4 (C and E) or 3 (G and I) cell pairs. Data from heteromeric cell pairs are plotted with filled symbols. The Gj/Vj plot for Inx2 homotypic channels (Fig. 1D) is included in each case for comparison (open symbols). Coexpression of *inx2* with each of the *vnx* RNAs induces the formation of intercellular channels that are sensitive to transjunctional voltage. (B and C) Inx2+VnxD. Cell pairs coinjected with *inx2* and *vnxD* RNAs form channels with voltage sensitivity similar to that for Inx2 homotypic channels. (D and E) Inx2+VnxG. Channels formed in cell pairs coexpressing *inx2* and *vnxG* are significantly less sensitive to applied Vjs than Inx2 homotypic channels. (F and G) Inx2+VnxQ1. Channels formed in cell pairs coexpressing *inx2* and *vnxQ1* show similar sensitivity to hyperpolarizing Vjs but greater sensitivity to depolarizing Vjs than Inx2 homotypic channels. (H and I) Inx2+VnxQ2. Channels in cell pairs coexpressing *inx2* and *vnxQ2* have a voltage profile similar to that of Inx2 homotypic channels.

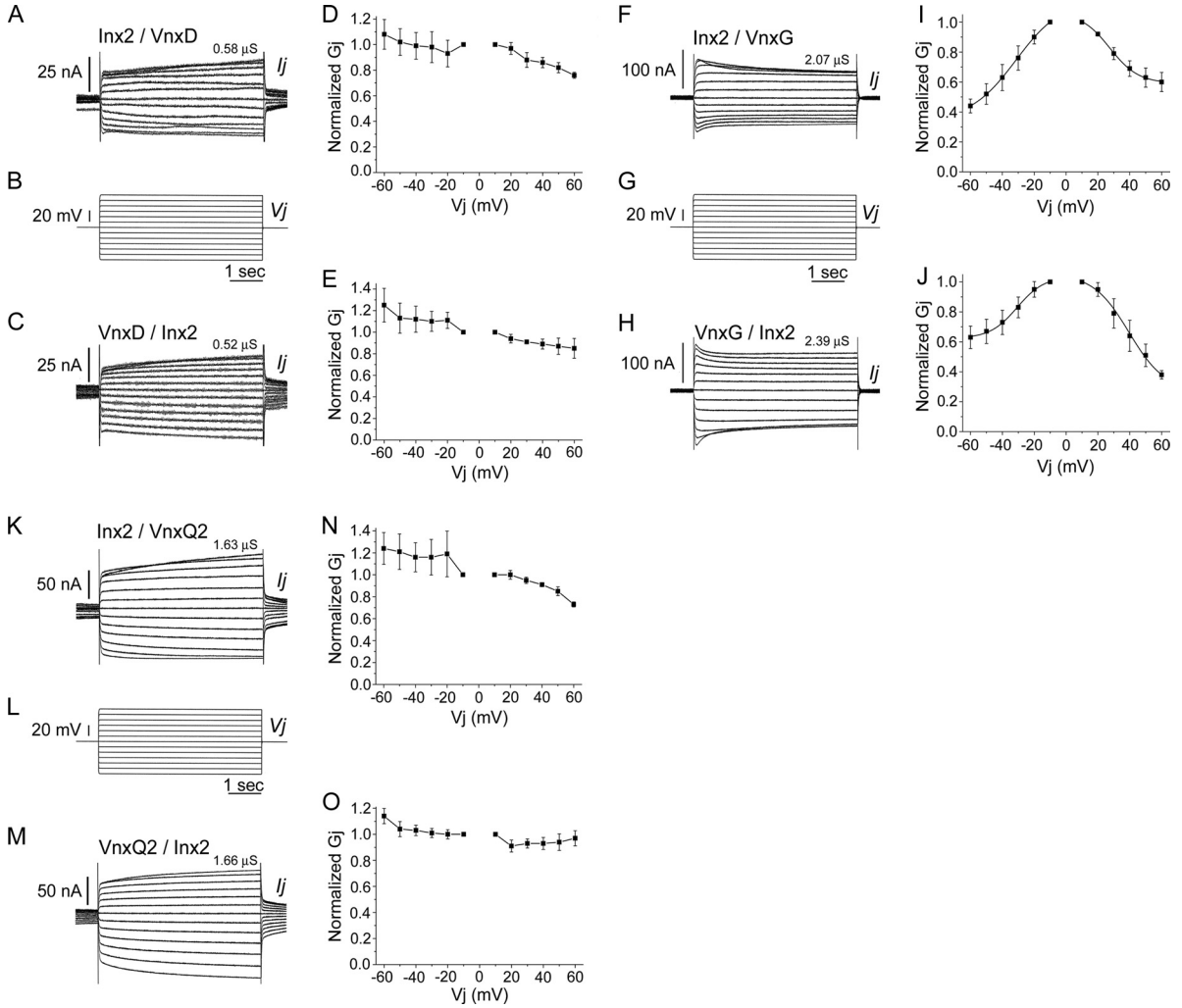

FIG. 4. *Sf*-Inx2 and the CsIV vinnexins form heterotypic gap junction channels. Cells injected with *Sf-inx2* RNA (2 ng) were paired with cells injected with one of the *CsIV-vnx* RNAs (10 ng), and cell pairs were recorded by dual voltage clamp as described in the legend for Fig. 1. Representative traces and corresponding Gj/Vj plots are shown for Inx2/VnxD (A to E), Inx2/VnxG (F to J), and Inx2/VnxQ2 (K to O). Each cell pair was recorded in both directions: stepping the Inx2-expressing cell through a series of hyperpolarizing and depolarizing voltages while recording induced currents in the Vnx-expressing cell (upper traces) and stepping the Vnx-expressing cell and recording currents in the Inx2-expressing cell (lower traces). In Gj/Vj plots, Gjs (mean ± SEM for 3 cell pairs, except panel J, where $n = 2$ for Vj of 60 mV) are normalized to their values at ±10 mV. Curves in panels I and J are Boltzmann fits of the data. (A to E) Inx2/VnxD. Inx2 forms heterotypic channels with VnxD that are weakly sensitive to transjunctional voltages; Gj tends to decline upon depolarization and increase upon hyperpolarization of either cell. (F to J) Inx2/VnxG. Inx2 and VnxG form heterotypic channels that respond asymmetrically to applied voltages; normalized Gjs decline to 40% of their maximum value when the Inx2-expressing cell is progressively hyperpolarized (F, G, and I) or the VnxG-expressing cell is progressively depolarized (G, H, and J). The decline in Gj is less steep when depolarizing Vjs are applied to the Inx2-expressing cell (F, G, and I) or hyperpolarizing Vjs are applied to the VnxG-expressing cell (G, H, and J). (K to O) Inx2/VnxQ2. Inx2 and VnxQ2 form heterotypic channels that are weakly voltage sensitive; Vj-dependent changes in Gj are observed when the Inx2-expressing cell is stepped (K, L, and N) but not when the VnxQ2-expressing cell is stepped (L, M, and O).

***Sf*-Inx2 forms heterotypic gap junction channels with the CsIV vinnexin proteins.** To investigate the likely contribution of heterotypic channels to the coupling observed in cell pairs in which both cells expressed both *Sf*-Inx2 and a CsIV-Vnx protein (Fig. 3), a series of experiments was carried out to investigate potential heterotypic channel formation between Inx2 and each of the vinnexins. For these experiments, oocytes were microinjected with either *inx2* mRNA (2 ng) or one of the *vnx* mRNAs (10 ng). Cells were then paired in a heterotypic configuration, each pair comprising an *inx2*-injected cell and a *vnx*-injected cell. The recordings revealed that Inx2 is able to form heterotypic gap junctions, to some extent, with all four Vnx proteins. The percentage of pairs coupled ranged from 13% for Inx2/VnxQ1 pairs to 92% for Inx2/VnxG pairs (Table 1). Representative recordings and corresponding Gj/Vj plots are shown for Inx2/VnxD, Inx2/VnxG, and Inx2/VnxQ2 heterotypic pairs (Fig. 4). In each case, the upper trace shows the response to application of voltage steps to the Inx2-expressing cell and the lower trace shows the response to voltage steps applied to the Vnx-expressing cell. Gj values (mean ± SEM), calculated at a Vj of ±10 mV and averaged from the recordings obtained in both directions for each pair, were 0.94 ± 0.24

μS ($n = 5$) for Inx2/VnxD pairs, 12.48 ± 3.68 μS ($n = 12$) for Inx2/VnxG pairs, and 0.82 ± 0.37 μS ($n = 5$) for Inx2/VnxQ2 pairs (Fig. 4; Table 1).

Inx2/VnxD heterotypic pairs (Fig. 4A to E) were weakly voltage sensitive. Gj declined slightly when depolarizing Vj steps of ≥20 mV were applied either to the Inx2-expressing cell (Fig. 4D) or to the VnxD-expressing cell (Fig. 4E); the drop in conductance was more marked when the Inx2-expressing cell was stepped. Application of hyperpolarizing Vj steps to either cell of the pair tended to increase Gj (Fig. 4). Inx2/VnxG heterotypic pairs (Fig. 4F to J) displayed clear voltage sensitivity. Gj decreased with increasing hyperpolarizing or depolarizing Vjs applied to either cell of the pair. The decline in Gj was steeper for hyperpolarization than for depolarization of the Inx2-expressing cell (Fig. 4I), whereas the opposite was true when the step protocol was applied to the cell expressing VnxG (Fig. 4J). The data fitted to a single Boltzmann equation. Gj_{max}, Gj_{min}, and V0 were 1.15 ± 0.37, 0.34 ± 0.27, and −31.38 ± 10.15, respectively, when the Inx2-expressing cell was hyperpolarized and 1.06 ± 0.18, 0.59 ± 0.08, and 27.48 ± 6.97, respectively, when this cell was depolarized (Fig. 4I). When the VnxG-expressing cell was stepped, values of Gj_{max}, Gj_{min}, and V0 were 1.04 ± 0.14, 0.62 ± 0.10, and −30.75 ± 7.73 for hyperpolarizing Vjs, with corresponding values of 1.06 ± 0.11, 0.27 ± 0.21, and 39.51 ± 7.35 for depolarizing Vjs (Fig. 4J). Inx2/VnxQ2 heterotypic pairs (Fig. 4K to O) were weakly voltage sensitive. Gj declined when the Inx2-expressing cell was depolarized; hyperpolarization of this cell had little effect on Gj (Fig. 4N). Application of either depolarizing or hyperpolarizing Vj steps to the VnxQ2-expressing cell did not significantly alter Gj (Fig. 4O). Heterotypic channel formation was observed in only one of eight Inx2/VnxQ1 pairs tested (recording not shown), with a Gj of 1.23 μS (Table 1).

DISCUSSION

Polydnaviruses are unique in their role as obligate symbiotic manipulators of host physiology, particularly immunity, in parasitoid-host systems. Their genomes reflect the selective advantages to be gained by manipulating the host, including methods to regulate viral gene expression in the parasitized host in the absence of replication, presence of several multigene families, and use of host homologues to affect host systems (55, 59). The last include vankyrins, homologues of NF-κB inhibitor (IκB) proteins, in both PDV lineages, the bracovirus protein tyrosine phosphatases (PTPs), and the ichnovirus vinnexins. Interestingly, while both the vankyrins and PTPs represent partial homologues, lacking clearly distinguished regulatory regions (60), the vinnexins are full-length homologues of insect gap junction proteins (54). This raises the distinct possibility that altered intercellular communication may underlie their effects on the physiology of parasitized hosts.

Virus and host lepidopteran innexins form gap junctions independently and interact to form junctions with novel properties *in vitro*. The data presented here demonstrating that CsIV VnxQ1 and VnxQ2 induce the formation of intercellular channels in paired *Xenopus* oocytes, together with our previous expression studies of CsIV-VnxG and CsIV-VnxD (54), establish that all four members of the CsIV Vnx gene family encode functional gap junction proteins. While the levels of conductance and percentages of homomeric cell pairs coupled vary (VnxG > VnxQ2 > VnxD > VnxQ1), Vnx channels have in common a lack of observable voltage sensitivity.

To explore possible interactions between Vnxs and their cellular homologues, we coexpressed the Vnxs with Inx2 from *Spodoptera frugiperda*. Inx2 was chosen for a number of reasons. Relative to other Inxs, this protein has the highest amino acid sequence identity with Vnxs (54) and may represent one of the innexins co-opted by the viruses during evolution. Inx2 also is transcribed in insect hemocytes (30, 44), the major immune cells of caterpillars. *Sf*-Inx2, which is the first lepidopteran innexin to be functionally expressed, reliably induced homotypic channels with voltage sensitivity similar to that for channels composed of the *Drosophila melanogaster* orthologue *Dm*-Inx2 (50).

Our Inx-Vnx coexpression studies provide convincing evidence of functional interactions between Inx2 and the Vnxs. Expression of Inx2 with VnxG or VnxQ1 in both oocytes of a pair resulted in the formation of channels with voltage properties (and, in the case of VnxQ1, also conductance properties) distinct from those of homotypic channels composed of either protein alone. This is consistent with these proteins forming heteromeric channels, in which individual hemichannels are composed of Inx2 and a Vnx, or heterotypic channels, in which one hemichannel is composed of Inx2 and the apposed hemichannel of a Vnx. Direct analysis of heterotypic interactions revealed that Inx2 and VnxG reliably form channels in this configuration. The voltage profile of these channels differed from that of channels in cells coexpressing both proteins, suggesting that Inx2 and VnxG assemble heteromeric, as well as heterotypic, channels. VnxQ1 and Inx2 also formed heterotypic channels with voltage properties distinct from those of channels in cell pairs coexpressing both proteins. However, the strength and reliability of coupling in heterotypic pairs were significantly lower than those in Inx2-VnxQ1 heteromeric pairs, and hence these proteins may preferentially assemble heteromeric channels. In contrast to VnxG and VnxQ1, coexpression of VnxD with Inx2 in both cells of a pair resulted in only subtle changes in voltage sensitivity. This makes it more difficult to evaluate in the oocyte expression system whether these proteins assemble heteromeric channels. The slight discrepancy between Inx2 homotypic pairs and Inx2+VnxD pairs in response to depolarizing potentials conceivably could be accounted for if the latter expressed a small population of heterotypic Inx2-VnxD channels (which we have shown form with low frequency) alongside homotypic Inx2 channels. The mean junctional conductance of Inx2+VnxD pairs, however, was significantly lower than that of Inx2 homotypic pairs. Arguably, a reduction in conductance may arise because of competition for translation or for transport of proteins to, and insertion into, the plasma membrane in cells coexpressing two exogenous RNAs. This seems unlikely here because expression of the same amounts of other Vnxs (VnxG and VnxQ2) with Inx2 did not affect mean Gj. In preliminary studies in cultured lepidopteran Sf9 and High Five cells, Inx2 exhibited similar subcellular distributions in the presence and absence of VnxD (D. K. Hasegawa and M. W. Turnbull, unpublished data). A reasonable conclusion, therefore, is that Inx2 and VnxD assemble heteromeric channels with lower conductance than

Inx2 homotypic channels. Our data provide no clear evidence for a heteromeric interaction between Inx2 and VnxQ2, but the proteins were found to interact in heterotypic configuration.

How might Vnxs act *in vivo* in host-parasitoid systems? We have demonstrated that Inx2 and Vnxs form gap junctions in an *in vitro* expression system. Can we extrapolate from this system to the whole organism? Studies of *Drosophila* and *Caenorhabditis elegans* innexins have demonstrated very good correspondence between the behavior of the proteins *in vitro* and *in vivo*. *Drosophila* ShakB(Neural+16) forms homotypic junctions and interacts with ShakB(Lethal) to form heterotypic junctions in *Xenopus* oocytes; in the fly, these proteins form homotypic and heterotypic junctions between specific neurons of the giant fiber system (41, 42). *Dm*-Inx2 and *Dm*-Inx3 cooperatively regulate epithelial tissue morphogenesis in the fly, consistent with their ability to form heteromeric channels *in vitro* (34, 50). *C. elegans* UNC-7S and UNC-9 form heterotypic junctions in *Xenopus* oocytes and between identified locomotory neurons in the worm (49). With these considerations in mind, the *in vitro* work presented here provides strong grounds for accepting that Vnxs form *de novo* gap junctions and/or interact with innexins to alter the properties of existing cellular junctions in host tissues.

Gap junctions are widely distributed in insect tissues (29, 51), and CsIV *vnx* genes are transcribed in several tissues of infected hosts (54). In principle, therefore, parasitic infection could result in altered intercellular communication in various physiological systems. A major factor in successful parasitization is suppression of the host's immune system. In immunocompetent lepidopterans, hemocytes wall off and kill invading parasites by forming a multilayered capsule around them (39). Morphological and electrophysiological studies of this encapsulation reaction have demonstrated the presence of hemocytic gap junctions (2, 8, 9, 27), which are hypothesized to function in capsule formation (8, 9, 26). Although the identity of the protein(s) that composes these junctions has not been established, Inx2 is a candidate, as the RNA is expressed in hemocytes (44). In CsIV-infected larvae, encapsulation may be initiated but not completed (15). It is conceivable that this disruption of capsule formation is Vnx mediated, as the genes are transcribed in, and at least one protein localizes to the membrane of, infected hemocytes (54).

While inhibition of encapsulation is a major factor in successful parasitization, other physiological processes also are disrupted. CsIV infection affects the endocrine system, notably causing prothoracic gland degeneration and reduced ecdysteroid titer (17, 18, 19, 45, 46, 57), although the viral factors responsible are unknown. Gap junctions are observed in insect endocrine tissues, including the larval lepidopteran prothoracic gland (14, 37, 43). It could be that Vnxs, if expressed in the gland of infected organisms, contribute to the hypothesized cell death underlying degeneration (19), for example, by altering cellular homeostasis or sensitivity to extrinsic regulatory signals. Additionally, multiple nutritional and developmental pathologies are induced by CsIV infection. While reduced translation of arylphorin and other hemolymph proteins is likely due to CsIV cys motif proteins (17, 18, 45, 46, 57), loss of cellular homeostasis due to disruption of typical gap junctional communication in the midgut (3, 4) or Malpighian tubules (61) could feasibly alter hemolymph composition.

In conclusion, our data prompt interesting hypotheses on the mechanism of action of ichnovirus-encoded vinnexins. Further experimental tools are required to test these hypotheses in the parasitoid-host system. Antibodies to Vnx proteins and lepidopteran Inxs, not yet available, will be essential to examine the relative distribution of the proteins in infected organisms. It will be important to develop means of manipulating Inx levels so that the effects of the parasite, or more specifically the Vnxs, on tissues over- or underexpressing gap junctions can be examined. At present, techniques for targeted manipulation of gene expression in lepidopterans are not well established. Translating the work into a more genetically tractable model, notably, *Drosophila melanogaster* (20), would provide an alternative approach.

ACKNOWLEDGMENTS

Work in this study was supported by a grant from the U.S. Department of Agriculture National Research Initiative (2006-03787) to M.W.T., a Clemson University Public Services Activities Next Generation Fellowship to D.K.H., and a BBSRC-sponsored Daphne Jackson Trust Fellowship to N.K.M., hosted by P.P.

We thank Sarah Reed for technical support.

REFERENCES

1. **Ayad, W. A., D. Locke, I. V. Koreen, and A. L. Harris.** 2006. Heteromeric, but not homomeric, connexin channels are selectively permeable to inositol phosphates. J. Biol. Chem. **281:**16727–16739.
2. **Baerwald, R. J.** 1975. Inverted gap and other cell junctions in cockroach hemocyte capsules: a thin section and freeze-fracture study. Tissue Cell **7:**575–585.
3. **Baldwin, K. M., R. S. Hakim, and G. B. Stanton.** 1993. Cell-cell communication correlates with pattern formation in molting *Manduca* midgut epithelium. Dev. Dyn. **197:**239–243.
4. **Bauer, R., C. Lehmann, and M. Hoch.** 2001. Gastrointestinal development in the *Drosophila* embryo requires the activity of innexin gap junction channel proteins. Cell Commun. Adhes. **8:**307–310.
5. **Beckage, N. E.** 1998. Modulation of immune responses to parasitoids by polydnaviruses. Parasitology **116:**S57–S64.
6. **Bezier, A., et al.** 2009. Polydnaviruses of braconid wasps derive from an ancestral nudivirus. Science **323:**926–930.
7. **Bruzzone, R., S. G. Hormuzdi, M. T. Barbe, A. Herb, and H. Monyer.** 2003. Pannexins, a family of gap junction proteins expressed in brain. Proc. Natl. Acad. Sci. U. S. A. **100:**13644–13649.
8. **Caveney, S., and R. Berdan.** 1982. Selectivity in junctional coupling between cells of insect tissues, p. 434–465. *In* R. C. King and H. Akai (ed.), Insect ultrastructure, vol. 1. Plenum Press, New York, NY.
9. **Churchill, D., S. Coodin, R. R. Shivers, and S. Caveney.** 1993. Rapid *de novo* formation of gap junctions between insect hemocytes *in vitro*: a freeze-fracture, dye-transfer and patch-clamp study. J. Cell Sci. **104:**763–772.
10. **Colman, A.** 1984. Translation of eukaryotic mRNA in *Xenopus* oocytes, p. 271–302. *In* B. D. Hames and S. J. Higgins (ed.), Transcription and translation—a practical approach. IRL, Oxford, United Kingdom.
11. **Cottrell, G. T., and J. M. Burt.** 2005. Functional consequences of heterogeneous gap junction channel formation and its influence in health and disease. Biochim. Biophys. Acta **1711:**126–141.
12. **Cui, L., A. I. Soldevila, and B. A. Webb.** 2000. Relationships between polydnavirus gene expression and host range of the parasitoid wasp *Campoletis sonorensis.* J. Insect Physiol. **46:**1397–1407.
13. **Curtin, K., Z. Zhang, and R. Wyman.** 2002. Gap junction proteins are not interchangeable in development of neural function in the *Drosophila* visual system. J. Cell Sci. **115:**3379–3388.
14. **Dai, J., M. J. Costello, and L. E. Gilbert.** 1994. The prothoracic glands of *Manduca sexta*: a microscopic analysis of gap junctions and intercellular bridges. Invertebr. Reprod. Dev. **25:**93–110.
15. **Davies, D. H., and S. B. Vinson.** 1988. Interference with function of plasmatocytes of *Heliothis virescens in vivo* by calyx fluid of the parasitoid *Campoletis sonorensis*. Cell Tissue Res. **251:**467–475.
16. **Desjardins, C. A., et al.** 2008. Comparative genomics of mutualistic viruses of *Glyptapanteles* parasitic wasps. Genome Biol. **9:**R183.
17. **Dover, B. A., D. H. Davies, and S. B. Vinson.** 1988. Degeneration of last instar *Heliothis virescens* prothoracic glands by *Campoletis sonorensis* polydnavirus. J. Invertebr. Pathol. **51:**80–91.

18. **Dover, B. A., D. H. Davies, and S. B. Vinson.** 1988. Dose-dependent influence of *Campoletis sonorensis* polydnavirus on the development and ecdysteroid titers of last-instar *Heliothis virescens* larvae. Arch. Insect Biochem. Physiol. **8:**113–126.
19. **Dover, B. A., T. Tanaka, and S. B. Vinson.** 1995. Stadium-specific degeneration of host prothoracic glands by *Campoletis sonorensis* calyx fluid and its association with host ecdysteroid titers. J. Insect Physiol. **41:**947–955.
20. **Duchi, S., et al.** 2010. The impact on microtubule network of a bracovirus IKB-like protein. Cell. Mol. Life Sci. **67:**1699–1712.
21. **Dupuy, C., E. Huguet, and J. M. Drezen.** 2006. Unfolding the evolutionary story of polydnaviruses. Virus Res. **117:**81–89.
22. **Dykes, I. M., F. M. Freeman, J. P. Bacon, and J. A. Davies.** 2004. Molecular basis of gap junctional communication in the CNS of the leech *Hirudo medicinalis*. J. Neurosci. **24:**886–894.
23. **Frank, M., et al.** 2010. Neuronal connexin-36 can functionally replace connexin-45 in mouse retina but not in the developing heart. J. Cell Sci. **123:** 3605–3615.
24. **Fushiki, D., Y. Hamada, R. Yoshimura, and Y. Endo.** 2010. Phylogenetic and bioinformatic analysis of gap junction-related proteins, innexins, pannexins and connexins. Biomed. Res. **31:**133–142.
25. **Glatz, R. V., S. Asgari, and O. Schmidt.** 2004. Evolution of polydnaviruses as insect immune suppressors. Trends Microbiol. **12:**545–554.
26. **Gupta, A. P.** 1991. Gap cell junctions, cell adhesion molecules, and molecular basis of encapsulation, p. 133–167. *In* A. P. Gupta (ed.), Immunology of insects and other arthropods. CRC Press, Boca Raton, FL.
27. **Han, S. S., and A. P. Gupta.** 1989. Arthropod immune system. II. Encapsulation of implanted nerve cord and "plain gut" surgical suture by granulocytes of *Blattella germanica* (L.) (Dictyoptera: Blattellidae). Zoolog. Sci. (Tokyo) **6:**303–320.
28. **He, D. S., J. X. Jiang, S. M. Taffet, and J. M. Burt.** 1999. Formation of heteromeric gap junction channels by connexins 40 and 43 in vascular smooth muscle cells. Proc. Natl. Acad. Sci. U. S. A. **96:**6495–6500.
29. **Hong, S. M., et al.** 2008. Two gap junction (innexin) genes of the *Bombyx mori* and their expression. J. Insect Physiol. **54:**180–191.
30. **Irving, P., et al.** 2005. New insights into *Drosophila* larval haemocyte functions through genome-wide analysis. Cell. Microbiol. **7:**335–350.
31. **Kroemer, J. A., and B. A. Webb.** 2006. Divergences in protein activity and cellular localization within the *Campoletis sonorensis* ichnovirus vankyrin family. J. Virol. **80:**12219–12228.
32. **Kroemer, J. A., and B. A. Webb.** 2005. IKB-related vankyrin genes in the *Campoletis sonorensis* ichnovirus: temporal and tissue-specific patterns of expression in parasitized *Heliothis virescens* lepidopteran hosts. J. Virol. **79:**7617–7628.
33. **Lapointe, R., et al.** 2007. Genomic and morphological features of a banchine polydnavirus: a comparison with bracoviruses and ichnoviruses. J. Virol. **81:**6491–6501.
34. **Lehmann, C., et al.** 2006. Heteromerization of innexin gap junction proteins regulates epithelial tissue organization in *Drosophila*. Mol. Biol. Cell **17:** 1676–1685.
35. **Li, S., J. A. Dent, and R. Roy.** 2003. Regulation of intermuscular electrical coupling by the *Caenorhabditis elegans* innexin inx-6. Mol. Biol. Cell **14:**2630–2644.
36. **Li, X., and B. A. Webb.** 1994. Apparent functional role for a cysteine-rich polydnavirus protein in suppression of the insect cellular immune response. J. Virol. **68:**7482–7489.
37. **Lococo, D. J., C. S. Thompson, and S. S. Tobe.** 1986. Intercellular communication in an insect endocrine gland. J. Exp. Biol. **121:**407–419.
38. **Luo, K., and M. W. Turnbull.** 2008. Manipulations of host cell physiology by polydnaviruses, p. 93–115. *In* N. Liu (ed.), Recent advances in insect physiology, toxicology, and molecular biology. Research Signpost, Kerala, India.
39. **Pech, L. L., and M. R. Strand.** 1996. Granular cells are required for encapsulation of foreign targets by insect haemocytes. J. Cell Sci. **109:**2053–2060.
40. **Phelan, P.** 2005. Innexins: members of an evolutionarily conserved family of gap-junction proteins. Biochim. Biophys. Acta **1711:**225–245.
41. **Phelan, P., et al.** 2008. Molecular mechanism of rectification at identified electrical synapses in the *Drosophila* giant fiber system. Curr. Biol. **18:**1955–1960.
42. **Phelan, P., et al.** 1998. *Drosophila* Shaking-B protein forms gap junctions in paired *Xenopus* oocytes. Nature **391:**181–184.
43. **Pow, D. V., and D. W. Golding.** 1989. Intercellular junctions in the corpora cardiaca of locusts. Cell Tissue Res. **258:**585–591.
44. **Shelby, K. S., and H. J. Popham.** 2009. Analysis of ESTs generated from immune-stimulated hemocytes of larval *Heliothis virescens.* J. Invertebr. Pathol. **101:**86–95.
45. **Shelby, K. S., and B. A. Webb.** 1994. Polydnavirus infection inhibits synthesis of an insect plasma protein, arylphorin. J. Gen. Virol. **75:**2285–2292.
46. **Shelby, K. S., and B. A. Webb.** 1997. Polydnavirus infection inhibits translation of specific growth-associated host proteins. Insect Biochem. Mol. Biol. **27:**263–270.
47. **Shelby, K. S., and B. A. Webb.** 1999. Polydnavirus-mediated suppression of insect immunity. J. Insect Physiol. **45:**507–514.
48. **Spray, D. C., A. L. Harris, and M. V. Bennett.** 1981. Equilibrium properties of a voltage-dependent junctional conductance. J. Gen. Physiol. **77:**77–93.
49. **Starich, T. A., J. Xu, I. M. Skerrett, B. J. Nicholson, and J. E. Shaw.** 2009. Interactions between innexins UNC-7 and UNC-9 mediate electrical synapse specificity in the *Caenorhabditis elegans* locomotory nervous system. Neural Dev. **4:**16.
50. **Stebbings, L. A., M. G. Todman, P. Phelan, J. P. Bacon, and J. A. Davies.** 2000. Two *Drosophila* innexins are expressed in overlapping domains and cooperate to form gap-junction channels. Mol. Biol. Cell **11:**2459–2470.
51. **Stebbings, L. A., et al.** 2002. Gap junctions in *Drosophila*: developmental expression of the entire innexin gene family. Mech. Dev. **113:**197–205.
52. **Swenson, K. I., J. R. Jordan, E. C. Beyer, and D. L. Paul.** 1989. Formation of gap junctions by expression of connexins in *Xenopus* oocyte pairs. Cell **57:**145–155.
53. **Tanaka, K., et al.** 2007. Shared and species-specific features among ichnovirus genomes. Virology **363:**26–35.
54. **Turnbull, M. W., A.-N. Volkoff, B. A. Webb, and P. Phelan.** 2005. Functional gap-junction genes are encoded by insect viruses. Curr. Biol. **15:**R491–R492.
55. **Turnbull, M. W., and B. A. Webb.** 2002. Perspectives on polydnavirus origins and evolution. Adv. Virus Res. **58:**203–254.
56. **Verselis, V. K., M. V. Bennett, and T. A. Bargiello.** 1991. A voltage-dependent gap junction in *Drosophila melanogaster*. Biophys. J. **59:**114–126.
57. **Vinson, S. B.** 1990. Physiological interactions between the host genus *Heliothis* and its guild of parasitoids. Arch. Insect Biochem. Physiol. **13:**63–81.
58. **Volkoff, A. N., et al.** 2010. Analysis of virion structural components reveals vestiges of the ancestral ichnovirus genome. PLoS Pathog. **6:**e1000923.
59. **Webb, B. A., and M. R. Strand.** 2005. The biology and genomics of polydnaviruses, p. 260–323. *In* L. I. Gilbert, K. Iatrou, and S. S. Gill (ed.), Comprehensive molecular insect science, vol. 5. Elsevier Press, San Diego, CA.
60. **Webb, B. A., et al.** 2006. Polydnavirus genomes reflect their dual roles as mutualists and pathogens. Virology **347:**160–174.
61. **Weng, X. H., et al.** 2008. Gap junctions in Malpighian tubules of *Aedes aegypti*. J. Exp. Biol. **211:**409–422.
62. **White, T. W.** 2002. Unique and redundant connexin contributions to lens development. Science **295:**319–320.
63. **White, T. W., R. Bruzzone, S. Wolfram, D. L. Paul, and D. A. Goodenough.** 1994. Selective interactions among the multiple connexin proteins expressed in the vertebrate lens: the second extracellular domain is a determinant of compatibility between connexins. J. Cell Biol. **125:**879–892.
64. **White, T. W., and D. L. Paul.** 1999. Genetic diseases and gene knockouts reveal diverse connexin functions. Annu. Rev. Physiol. **61:**283–310.
65. **Wolfle, S. E., et al.** 2007. Connexin45 cannot replace the function of connexin40 in conducting endothelium-dependent dilations along arterioles. Circ. Res. **101:**1292–1299.
66. **Yen, M. R., and M. H. Saier, Jr.** 2007. Gap junctional proteins of animals: the innexin/pannexin superfamily. Prog. Biophys. Mol. Biol. **94:**5–14.
67. **Yum, S. W., et al.** 2007. Human connexin26 and connexin30 form functional heteromeric and heterotypic channels. Am. J. Physiol. Cell Physiol. **293:** C1032–C1048.
68. **Zheng-Fischhofer, Q., et al.** 2006. Connexin31 cannot functionally replace connexin43 during cardiac morphogenesis in mice. J. Cell Sci. **119:**693–701.